



euronoise

# Acoustic microelectromechanical viscometer

Arthur Ballato

US Army Communications-Electronics R&D Center, AMSRD-CER-CS, Fort Monmouth, NJ 07703-5201, USA
arthur.ballato@us.army.mil

Current dynamic techniques for measuring fluid shear viscosities using quartz, or other piezoelectrics, rely on the resonator surface being exposed to a measurand bath whose extent greatly exceeds the penetration depth of the evanescent shear mode excited by the active element. This configuration allows the effect of the loading parameters to be expressed concisely. Perturbation of the electrical equivalent circuit parameters of the resonator by the fluid loading permits calculation of the mass density – shear viscosity product. In this paper, we explore the interesting, albeit more complicated situation where the separation between the resonator and a confining wall is less than the penetration depth of the fluid occupying the intervening region. It turns out that the resonator perturbation in this case is a sensitive function of the separation. This important fact permits extreme miniaturization, since for gases between 200°K and 400°K, pressures between 0.01 to 100 atm, and frequencies between 10 MHz and 1 GHz, the penetration depth varies from micrometers to nanometers. Variations in the spacing is effected by using a second, nonresonant piezoelectric as the wall. Micro-electro-mechanical (MEMS) versions of viscometers and associated types of fluid sensors are thereby enabled.

# 1 Introduction

Quimby originated the technique of measuring solids by attaching them to a quartz crystal [1]. The Quimby composite resonator (QCR) reduces to that of the quartz crystal microbalance (QCM) [2,3,4] in the limit where the measurand becomes a thin film, and its elasticity is neglected [5,6,7]. Mason first adapted the technique for measuring liquids [8,9,10]. This method remains very popular, e.g., [11,12,13,14,15,16,17]. References [7,13] contain many more pertinent citations. Stockbridge used the modality to measure gases [18,19]. In these applications, the crystal resonator is measured without, and then with, the loading of the measurand. Ensuing changes are registered as changes in frequency, phase, and/or impedance level, from which the unknown measurand properties are inferred.

# 2 Equivalent Electric Circuit

Over the years, many equivalent circuits have been used to model the piezoresonator, and to describe its behavior when its surface is subjected to various conditions of loading [20,21,22,23,24]. The most popular is the Butterworth–Van Dyke (BVD) network, consisting of a capacitance $C_0$, shunted by an $R_1$, $L_1$, and $C_1$ series arm [20]. The series arm is the manifestation of the piezoelectrically induced vibratory motion at a single isolated resonance. The BVD lumped circuit evolved into more elaborate broad-band, multi-mode, transmission-line networks that place the mechanical boundary loadings and piezoelectric excitation mechanism in series at the surfaces [22,23].

# 3 Fluid Loading

We consider one surface of the piezoelectric resonator to be in contact with a fluid to be measured. Lord Rayleigh, commenting on Stokes' treatment of fluid viscosity, wrote [25, §347]: "The velocity of the fluid in contact with the plane is usually assumed to be the same as that of the plane itself on the apparently sufficient ground that the contrary would imply an infinitely greater smoothness of the fluid with respect to the solid than with respect to itself." This assumption is implicit in the following treatment.

An unbounded Newtonian fluid, (i.e., a fluid with shear viscosity, $\eta$, in addition to the usual attributes of mass density, $\rho$, and elastic stiffnesses, $c_S$ and $c_L$), in intimate contact with a resonator surface of area A, presents to the surface both shear (S) and longitudinal (L) impedances. These depend on angular frequency, $\omega$. Mechanical shear impedance is $Z_S = A\sqrt{(j\omega\eta\rho)} = R_S + j\omega L_S$. $R_S$ represents shear dissipation, and $L_S$ models entrained mass loading. Penetration depth is $\delta = \lambda/2\pi = \sqrt{(2\eta/\rho\omega)}$. Longitudinal impedance consists of $R_L = A\rho v_L = A\sqrt{(\rho c_L)}$, representing energy radiating into the fluid, plus a small reactance representing wave attenuation; we neglect longitudinal viscosity. These impedances, transformed by a piezoelectric factor, appear in the BVD circuit in series with the $R_1$, $L_1$, $C_1$ branch [15,16]. Thus, immittance and/or frequency measurements on a resonator immersed in an unbounded fluid (i.e., when distance ($\ell$) from the resonator surface to a confining surface greatly exceeds the penetration depth, $\delta$), yield only the ($\rho c_L$) and ($\eta\rho$) products.

# 4 Confined Fluid Loading

For the great majority of fluids and ambient conditions and frequencies of interest, the penetration depth, $\delta$, characterizing the evanescent shear wave, ranges from micrometers to nanometers. We consider the effect of introducing a planar rigid boundary parallel to the surface of the piezoelectric resonator in order to confine the fluid therebetween. Fine adjustments to the spacing between the surfaces are easily accommodated by the use of a second piezoelectric element, or, e.g., an "inchworm" mechanism [26]. When the distance, $\ell$, separating the two surfaces becomes comparable to $\delta$, the formulas above no longer hold. Instead, the surface of the resonator sees a complex mechanical admittance of

$$A\cdot Y_S = A\cdot(G_S + jB_S) =$$

$$\sqrt{(j/2)}\cdot(\delta/\eta)\cdot\tan[\sqrt{(2/j)}\cdot(\ell/\delta)]. \quad (1)$$

The complex mechanical impedance is

$$Z_S = R_S + jX_S = 1/Y_S. \quad (2)$$

With the abbreviations $w = (\ell/\delta)$ and $p = (\delta/\eta)$, shear conductance, $G_S(w)$ and reactance $X_S(w)$ are:

$G_S = g(w)\cdot(p/A) = g(w)/[A\cdot\sqrt{(\omega\rho\eta/2)}]$, and (3)

$X_S = x(w)\cdot(A/p) = x(w)\cdot A\cdot\sqrt{(\omega\rho\eta/2)}$, where (4)

g(w) and x(w) are dimensionless factors with the general form of a tanh function with superposed cyclic modulation. Figures 1 and 2 show g(w) and x(w), respectively. The first three extrema of g(w) are 0.68111 at w = 0.9375, 0.49093 at w = 2.347 and 0.050039 at w = 3.929; g(0) = 0, and g(∞) = 1/2. The first extremum of x(w) is 1.0178 at w = 2.366; x(0) = 0, and x(∞) = 1. At w = 0, the slopes are: dg(0)/dw = +1, and dx(0)/dw = +2/3. Similarly defined factors, b(w), |y(w)|, r(w), |z(w)| behave as follows for w << 1: r(w) and |z(w)| are hyperbolic; |y(w)| is linear, and b(w) is zero, with zero slope.

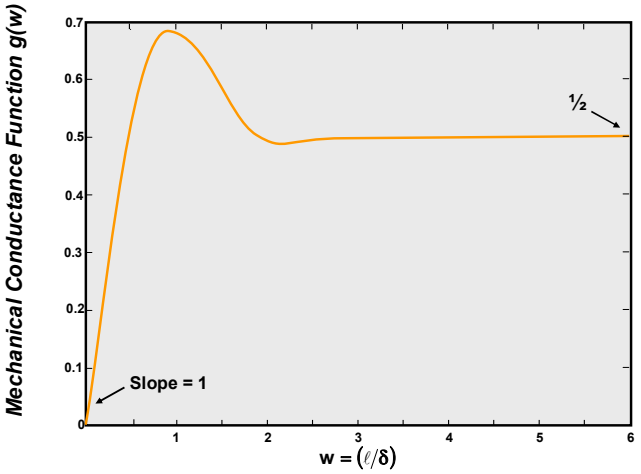


Fig. 1 Mechanical conductance function g(w).

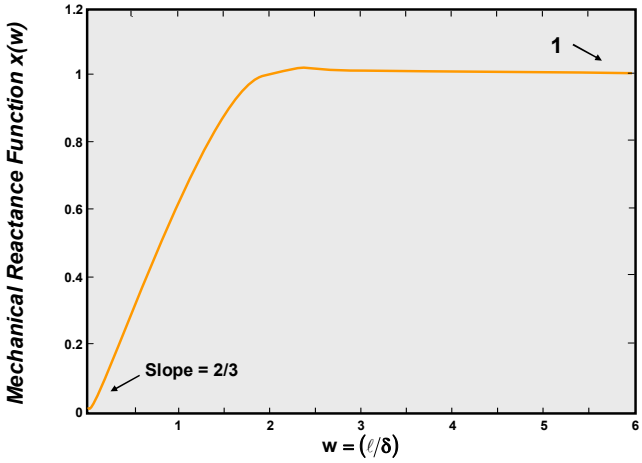


Fig. 2 Mechanical reactance function x(w).

## 5 Viscosity and Mass Density

When w << 1, g(w) ≈ [dg(w)/dw]·w ≈ w = (ℓ/δ), and viscosity η may be determined directly from the relation

$A\cdot\eta = (\Delta G_S/\Delta\ell)^{-1}$ (5)

Similarly,

$A\cdot\rho = (3/\omega)\cdot((\Delta X_S/\Delta\ell)$. (6)

Equations (5) and (6) express mechanical values. In order to convert them to electrical form, $G_S$ is multiplied, and $X_S$ is divided, by the factor $n^2 = (Ae/t)^2$, where e is an effective piezoelectric stress coefficient, and t the thickness of the resonator.

Thus, for w in the range where g(w) and x(w) are linear, automatic network analyzer measurements yield direct determinations of viscosity and mass density. As a check, the region w >> 1 provides the (ρη) product. Similar remarks pertain to use of longitudinal resonators to yield values of the compressional stiffness ($c_L$) directly. Because δ is usually very small, MEMS miniaturization is a natural consequence of using the w << 1 regime.

## 6 Some Numerical Values

Rayleigh [25, p.313] remarks: "Both by theory and experiment the remarkable conclusion has been established that within wide limits the force *[viscosity]* is independent of the density of the gas." Tables 1 and 2 contain values of pertinent acoustic properties of argon at 200° K, ($\eta = 2.125\ 10^{-5}$ Pa-s), and hydrogen at 400° K, ($\eta = 1.0867\ 10^{-5}$ Pa-s) [27,28]. In these tables and those below, the δ values are for a frequency of 1 MHz.

| Pressure | ρ | $R_S$ | δ |
|---|---|---|---|
| atm | kg/m$^3$ | kg/(s·m$^2$) | μm |
| 0.01 | 0.02434 | 1.115 | 14.58 |
| 0.1 | 0.24347 | 3.526 | 4.609 |
| 1 | 2.4411 | 11.163 | 1.456 |
| 10 | 25.087 | 35.787 | 0.4541 |
| 100 | 351.94 | 134.04 | 0.1212 |

Table 1 - Acoustic parameters of argon

| Pressure | ρ | $R_S$ | δ |
|---|---|---|---|
| atm | kg/m$^3$ | kg/(s·m$^2$) | μm |
| 0.01 | 0.00061419 | 0.145 | 75.05 |
| 0.1 | 0.0061419 | 0.458 | 23.73 |
| 1 | 0.061392 | 1.448 | 7.506 |
| 10 | 0.61131 | 4.568 | 2.379 |
| 100 | 5.8578 | 14.142 | 0.7684 |

Table 2 - Acoustic parameters of hydrogen

Tables 3 and 4 provide acoustic values for additional fluids. When dealing with miniaturized devices having fluid gaps in the order of micrometers to nanometers, one must take into account the deviations from Newtonian behavior due to finite atomic and molecular dimensions of the fluids. In addition, for gases at pressures below about ½ atm, viscoelastic behavior [18] is observed, and one must deal

with a complex viscosity having a relaxation frequency (Maxwell fluid); see also [13].

| $H_2O$/glycerol ($C_3H_8O_3$) | $\rho$ kg/m$^3$ | $v_L$ m/s | $\eta$ Pa · s | $\delta$ μm |
|---|---|---|---|---|
| volume % | | | | |
| 25% water | 1205 | 1738 | 0.046 | 3.486 |
| 20% water | 1217 | 1765 | 0.076 | 4.458 |
| 15% water | 1228 | 1798 | 0.13 | 5.805 |
| 10% water | 1239 | 1828 | 0.25 | 8.014 |
| 05% water | 1250 | 1870 | 0.58 | 12.15 |
| 00% water | 1260 | 1909 | 1.5 | 19.47 |

Table 3 - Acoustic parameters of $H_2O$/glycerol mixtures

| Substance | T °C | $\rho$ kg/m$^3$ | $\eta$ mPa-s | $\delta$ μm |
|---|---|---|---|---|
| water | 0 | 999.8 | 1.79 | 0.755 |
| water | 20 | 998.2 | 1.00 | 0.565 |
| water | 100 | 958.4 | 0.28 | 0.305 |
| vapor | 100 | 0.6 | 0.013 | 2.626 |
| whole blood | 37 | 1060 | 3.5 | 1.023 |
| ethyl alcohol | 20 | 789.20 | 1.15 | 0.680 |
| helium | 0 | 0.1786 | 18.6 | 5.758 |
| mercury | 15 | 13,550 | 1.55 | 0.191 |
| SAE 10 | 20 | 875 | 65 | 4.863 |
| SAE 20 | 20 | 885 | 125 | 6.705 |
| SAE 30 | 20 | 890 | 200 | 8.458 |
| SAE 40 | 20 | 900 | 319 | 10.622 |
| glycerine | 25 | 1258.02 | 1420 | 18.955 |

Table 4 - Acoustic parameters of various fluids

# 7 Conclusion

We have considered Newtonian fluids subjected to shear motion, in the limit where the distance to a confining rigid wall is comparable to the penetration depth. It is found that the immittance seen at the face of the shear transducer, (and reflected in the transducer equivalent electrical circuit values), permits direct determination separately of the viscosity and mass density. The smallness of the penetration depth, in most applications, is such that extreme miniaturization is thereby enabled.

# References

[1] S. L. Quimby, "On the experimental determination of the viscosity of vibrating solids," Phys. Rev. 25, 558-573 (1925)

[2] G. Sauerbrey, "Wägung dünner Schichten mit Schwingquarzen," Physikalische Verhandlungen, 8, 193 (1957)

[3] G. Sauerbrey, "Verwendung von Schwingquarzen zur Wägung dünner Schichten und zur Mikrowägung," Zeitschrift für Physik, 155, 206-222 (1959)

[4] P. Lostis, "Étude, réalisation et contrôle de lames minces introduisant une différence de marche déterminée entre deux vibrations rectangulaires," Part 2: "Nouvelle méthode de contrôle de l'epaisseur pendant l'évaporation," Revue d'optique, théorique et instrumentale, 38, 1-28 (1959)

[5] E. Benes, "Improved quartz crystal microbalance technique," J. Appl. Phys., 56, 608-626 (1984)

[6] H. Nowotny and E. Benes, "General one-dimensional treatment of the layered piezoelectric resonator with two electrodes," J. Acoust. Soc. Am., 82, 513-521 (1987)

[7] A. Ballato, "Compound resonators and microweighing sensors," IEEE Intl. Frequency Contr. Symp. Proc., 186-191 (2006)

[8] W. P. Mason, "Measurement of the viscosity and shear elasticity of liquids by means of a torsionally vibrating crystal," Trans. Am. Soc. Mech. Eng., 68, 359-370 (1947)

[9] W. P. Mason, "Viscosity and shear elasticity measurements of liquids by means of shear vibrating crystals," J. Colloid Sci. 3, 147-162 (1948)

[10] W. P. Mason, W. O. Baker, H. J. McSkimin, J. H. Heiss, "Measurement of shear elasticity and viscosity of liquids at ultrasonic frequencies," Phys. Rev., 75, 936-946 (1949)

[11] Z. Kojro, E.v.d. Burg, J. Zinke, K. Hillmann, W. Grill, "Viscosity shear waves and mass drag effects in liquids," Zeitschrift für Physik B 101, 433-439 (1996)

[12] Y. Kim, J. R. Vig, A. Ballato, "Sensing the properties of liquids with doubly rotated resonators," IEEE Intl. Freq. Contr. Symp. Proc., 660-666 (1998)

[13] A. Ballato, "Piezoelectric resonators loaded with viscoelastic and nonuniform media," IEEE Intl. Freq. Contr. Symp. Proc., 191-201 (2002)

[14] E. Benes, R. Thalhammer, M. Gröschl, H. Nowotny, S. Jary, "Viscosity sensor based on a symmetric dual quartz thickness shear resonator," IEEE Intl. Frequency Contr. Symp. & 17th Eur. Freq. and Time Forum Proc., 1048-1054 (2003)

[15] D. C. Ash, M. J. Joyce, C. Barnes, C. J. Booth, A. C. Jefferies, "Viscosity measurement of industrial oils using the droplet quartz crystal microbalance," Meas. Sci. Technol. 14, 1955-1962 (2003)

[16] A. Saluja, D. S. Kalonia, "Measurement of fluid viscosity at microliter volumes using quartz impedance analysis," AAPS PharmSciTech, 5, Art. 47 (2004)

[17] Y. Kim, J. R. Vig, A. Ballato, "Doubly rotated resonators for sensing the properties of liquids," IEEE Trans. Ultrason., Ferroelect., Freq. Contr. 51, 1388-1393 (2004)

[18] C. D. Stockbridge, "Effects of gas pressure on quartz-crystal microbalances," in Vacuum Microbalance Techniques, 5, 147-178 Plenum (1966)

[19] C. D. Stockbridge, "Effect of hydrostatic pressure on rotated Y-cut quartz crystal resonators," in Vacuum Microbalance Techniques, 5, 179-191 Plenum (1966)

[20] A. Ballato, "Resonance in piezoelectric vibrators," Proc. IEEE 58, 149-151 (1970)

[21] D. W. Dye, "The piezo-electric quartz resonator and its equivalent electrical circuit," Proc. Phys. Soc. (London), 38, 399-458 (1926)

[22] R. W. Cernosek, S. J. Martin, A. R. Hillman, H. L. Bandey, "Comparison of lumped-element and transmission-line models for thickness-shear-mode quartz resonator sensors," IEEE Intl. Freq. Contr. Symp. Proc., 96-104 (1997)

[23] A. Ballato, "Modeling piezoelectric and piezomagnetic devices and structures via equivalent networks," IEEE Trans. Ultrason., Ferroelect., Freq. Contr. 48, 1189-1240 (2001)

[24] U. Hempel, R. Lucklum, P. R. Haupmann, E. P. EerNisse, D. Puccio, R. F. Diaz, "Quartz crystal resonator sensors under lateral field excitation – A theoretical and experimental analysis," Meas. Sci. Technol. 19, art. 055201 (2008)

[25] J. W. S. Rayleigh, The Theory of Sound, Vol. 2, 2nd revised edition, (1896), Dover, New York (1945)

[26] P. E. Tenzer, R. B. Mrad, "A systematic procedure for the design of piezoelectric inchworm precision positioners," IEEE/ASME Trans. Mechatronics, 9, 427-435 (2004)

[27] J. Hilsenrath, C. W. Beckett, W. S. Benedict, L. Fano, H. L. Hoge, J. F. Masi, R. L. Nuttall, Y. S. Touloukian, and H. W. Woolley, "Tables of Thermal Properties of Gases," NBS Circular 564, National Bureau of Standards, Washington, DC (1955)

[28] J. Hilsenrath, "Thermodynamic Properties of Gases," in American Institute of Physics Handbook, 2nd ed., D. E. Gray, Ed., McGraw-Hill, New York (1963)